Available online at www.sciencedirect.com
SCIENCE DIRECT®
Spectrochimica Acta Part A 64 (2005) 681–692
SPECTROCHIMICA ACTA PART A
www.elsevier.com/locate/saa

Raman spectroscopy of diamondoids

Jacob Filik [a], Jeremy N. Harvey [a], Neil L. Allan [a], Paul W. May [a,*], Jeremy E.P. Dahl [b], Shenggao Liu [b], Robert M.K. Carlson [b]

[a] *School of Chemistry, University of Bristol, Bristol BS8 1TS, UK*
[b] *MolecularDiamond Technologies, ChevronTexaco Technology Ventures, Post Office Box 1627, Richmond, CA 94802, USA*

Received 11 July 2005; received in revised form 30 July 2005; accepted 30 July 2005

Abstract

A selection of diamondoid hydrocarbons, from adamantane to [121321] heptamantane, have been analysed by multi-wavelength laser Raman spectroscopy. Spectra were assigned using vibrational frequencies and Raman intensities were calculated by employing the B3LYP functional and the split valence basis set of Schafer, Horn and Ahlrichs with polarisation functions on carbon atoms. The variation of the spectra and associated vibrational modes with the structure and symmetry of the molecules are discussed. Each diamondoid was found to produce a unique Raman spectrum, allowing for easy differentiation between molecules. Using the peak assignments derived from the calculations we find that the low frequency region of the spectra, corresponding to CCC-bending/CC-stretching modes, is particularly characteristic of the geometric shape of the diamondoid molecules.

Keywords: Raman; Spectroscopy; Diamondoids; Polymantanes; Diamond hydrocarbons; Density functional theory

1. Introduction

Since the discovery of adamantane from petroleum in 1933 [1], there has been great interest in the properties of this once unique cage-structured molecule. Some years later it was joined by diamantane [2] to form the two smallest examples of a series of molecules known as “diamond hydrocarbons” or diamondoids. Synthetically, chemists managed to reproduce these structures in the laboratory [3] and go two steps further, producing both triamantane [4] and a tetramantane that bore structural resemblance to butane in its anti conformation [5]. For larger systems, the huge number of potential intermediates, reaction pathways, and complex reaction schemes has prevented the synthetic production of higher polymantanes [6].

In 2003, MolecularDiamond Technologies used vacuum distillation and a combination of chromatographic techniques to isolate a range of diamondoid molecules [7], again from petroleum. For the first time, diamondoids, from tetramantanes to an undecamantane, were available.

Use of the systematic von Baeyer nomenclature for polymantanes is somewhat counter-productive, with even the simple triamantane being correctly referred to as heptacyclo[7.7.$1^{3,15}$.$0^{1,12}$.$0^{2,7}$.$0^{4,13}$.$0^{6,11}$]octadecane. Luckily, with an impressive display of foresight, the problem of naming these newly discovered molecules was tackled in 1978 by Balaban and von Schleyer [8]. To avoid the adoption of a plethora of trivial names to categorize isomeric polymantanes, they used graph theory to formulate a manageable numerical prefix, based on the relative positions of the centres of the fused adamantane units. This prefix is followed by the Greek numeral for the number of adamantane units and the suffix “mantane”, e.g. [1(2,3)4] pentamantane. Without delving too deeply into the conventions of this classification, there are a few simple observations relevant to this paper. The smallest diameter “rod” of diamondoid has a prefix that consists solely of alternating ones and twos. For example [1212] pentamantane (Fig. 1(g)) is a “rod-shaped” diamondoid containing five adamantane units. Flat diamondoid molecules that just extend in two dimensions only have ones, twos and threes in their prefix, e.g. [12312] hexamantane (Fig. 1(n)) is a “disc-shaped” diamondoid containing six adamantanes. Following from this, when a prefix contains ones, twos, threes and fours, the diamondoid network is extended in all three dimensions, e.g. [1(2,3)4] pentamantane (Fig. 1(h)) is a tetrahedron made of five adamantane units. Only pentaman-

* Corresponding author. Tel.: +44 1173317555.
E-mail addresses: jacob.filik@bris.ac.uk (J. Filik), Paul.May@bris.ac.uk (P.W. May).
URL: http://www.chm.bris.ac.uk/pt/diamond..

1386-1425/$ – see front matter © 2005 Elsevier B.V. All rights reserved.
doi:10.1016/j.saa.2005.07.070

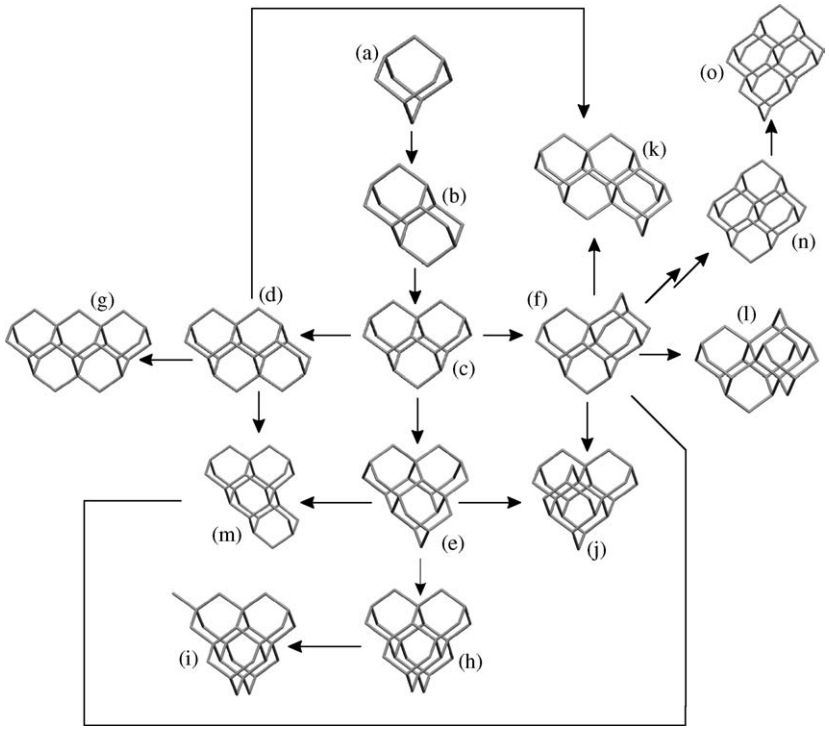

Fig. 1. Diamondoids studied in this experiment, (a) adamantane $C_{10}H_{16}$ T_d, (b) diamantane $C_{14}H_{20}$ D_{3d}, (c) triamantane $C_{18}H_{24}$ C_{2v}, (d) [121] tetramantane $C_{22}H_{28}$ C_{2h}, (e) [1(2)3] tetramantane $C_{22}H_{28}$ C_{3v}, (f) [123] tetramantane $C_{22}H_{28}$ C_2, (g) [1212] pentamantane $C_{26}H_{32}$ C_{2v}, (h) [1(2,3)4] pentamantane $C_{26}H_{32}$ T_d, (i) 3-methyl-[1(2,3)4] pentamantane $C_{27}H_{34}$ C_{3v}, (j) [12(3)4] pentamantane $C_{26}H_{32}$ C_s, (k) [1213] pentamantane $C_{26}H_{32}$ C_1, (l) [1234] pentamantane $C_{26}H_{32}$ C_2, (m) [12(1)3] pentamantane $C_{26}H_{32}$ C_1, (n) [12312] hexamantane $C_{26}H_{30}$ D_{3d}, (o) [121321] heptamantane $C_{30}H_{34}$ C_s.

tanes or larger can extend in three dimensions, tetramantanes are always flat and their prefix will only contain ones, twos or threes.

Laser Raman spectroscopy is a popular characterisation technique used to probe the structure of materials. The Raman spectra of adamantane and several of its derivatives have been studied on many occasions and in great detail [9,10]. These experiments were conducted on the solid phase and to a good approximation it was possible to divide modes into intramolecular and intermolecular.

The intramolecular studies concentrate on the high wavenumber region (above 300 cm^{-1}) of the spectrum and in general use theoretical calculations performed on a single molecule to assist with the mode assignment [11]. Very recently, Jensen [9] published a highly detailed assignment of the normal modes of vibration of both adamantane and deuterated adamantane, producing normal mode based empirical correction factors at the Hartree–Fock, DFT (B3LYP) and MP2 levels. In other work [10] attempts have been made to correlate the Raman spectra of adamantane and diamantane with that of nanocrystalline diamond. However, it is now widely accepted that any peaks found in the Raman spectrum of a chemical vapour deposition nanocrystalline diamond film, excluding the diamond 1332 cm^{-1} Brillouin zone centre mode, are due to non-diamond phases of carbon [12]. Adamantane derivatives also studied by this combination of Raman spectroscopy and computational methods include 2-adamantanone [11], 1,1′-biadamantane [13], perfluoroadamantane [14], and the antiparkinson drug amantadine [15]. To date the largest diamondoid to be analysed by Raman spectroscopy is [12312] hexamantane [16] (often referred to as cyclohexamantane), but the spectral assignment was based on semiempirical (AM1) calculations on adamantane, and is therefore not completely reliable. Despite there being very little experimental Raman data for other diamondoids, interest in the theoretical calculations of the molecular vibrational frequencies and Raman intensities is growing [17,18].

Conversely, intermolecular studies focus on the low wavenumber region (sub 300 cm^{-1}) and are concerned with the motion of molecular units in the crystal relative to each other. Such studies are usually performed over a range of temperatures to observe solid-solid phase transitions [19,20]. The most relevant example of this is the plastic transition in adamantane. At low temperature, crystalline adamantane has the space group D^4_{2d} with two molecules per primitive unit cell. Raising the temperature to above 209 K produces a phase transition to the plastic state. During this transition the sharp but weak low frequency lattice modes observed in the Raman spectrum become a broad wing [19], tentatively assigned to disorder-induced scattering in the Raman disallowed first-order spectrum of the high temperature structure.

We now present the first general study of the Raman spectra of a large family of diamondoids. In this investigation, the effects of variations in structure and symmetry on the intramolecular vibrations of a selection of diamondoid molecules, from adamantane to [121321] heptamantane (Fig. 1), are analysed by Raman spectroscopy. Assignments are made using vibrational frequencies and Raman intensities calculated at the B3LYP level of theory. Spectra are compared and contrasted with respect to

the molecular geometries of the diamondoids with special attention being paid to any modes that may be structurally diagnostic.

Fig. 1 depicts the relationships between all the diamondoids included in this study. The first three structures, adamantane (a), diamantane (b), and triamantane (c), are the only isomers possible constructed of one, two or three adamantane units. A further unit can be added in eight distinct ways, producing [121] tetramantane (d), [1(2)3] tetramantane (e), and both enantiomers of the chiral [123] tetramantane (f).

All the other diamondoids in this study are built by the addition of further adamantane units on the base of these four structures with the exception of (i) which results from methyl addition to (h). The pentamantanes can be split into two groups; those whose structure can only be related to a single tetramantane, and those whose structure is based on a combination of two or all three tetramantanes. The first group contains [1212] pentamantane (g), [1(2,3)4] pentamantane (h), and chiral [1234] pentamantane (l), whose structures are uniquely based on [121] tetramantane, [1(2)3] tetramantane and [123] tetramantane, respectively. There is predicted to be a further pentamantane, [1231] pentamantane, uniquely related to [123] tetramantane, which is the base pentamantane for [12312] hexamantane (n), but this has not yet been isolated, and may not even be stable due to steric interactions between two specific neighbouring hydrogens. The second group contains chiral [1213] pentamantane (k) (related to [121] and [123] tetramantanes), [12(3)4] pentamantane (j) (related to [123] and [1(2)3] tetramantanes) and chiral [12(1)3] pentamantane (m) (related to [121], [1(2)3] and [123] tetramantanes). This inherent ordering permits the grouping of this selection of diamondoids by their root tetramantane(s), producing five groups, adamantane to triamantane, then three groups uniquely derived from and including all tetramantanes, and finally pentamantanes that can be made by addition to either of two or all three tetramantanes. [12312] Hexamantane (n) and [121321] heptamantane (o) are analysed in their own section due to the absence of [1231] pentamantane that would help relate [12312] hexamantane to [123] tetramantane.

2. Experimental and computational details

Raman spectra were measured using Renishaw inVia (488 nm Ar^+, 2400 l/mm grating) and 2000 (514 nm Ar^+ laser, 785 nm diode laser, 1200 l/mm grating and 325 nm He–Cd laser, 2400 l/mm grating) spectrometers. No wavenumber dispersion was observed with the change in excitation wavelength. Changes in relative peak intensity were noticed, but are most likely attributable to the system response function of each spectrometer. All the spectra presented here were produced using the 488 nm system, chosen because of its superior resolution and flat system response function.

Spectra were studied in the range 200–3200 cm^{-1} and could be split into two distinct regions, the "CH stretch region" between 3100 and 2800 cm^{-1} and the "CH bend, CC stretch region" between 1600 and 200 cm^{-1}.

Diamondoid samples varied in size from small single crystals (sub 1 mm) to fine powders. Generally, the single crystals produced a superior spectrum, with a higher signal-to-noise ratio and lower luminescence. All chiral diamondoids were present as racemic mixtures.

Calculations were performed using Gaussian 03 [21], using the standard B3LYP functional and the split valence basis set of Schaefer et al. [22] with polarisation functions on carbon. Raman intensities were calculated by numerical differentiation of dipole derivatives with respect to the electric field.

3. Results

The experimental and calculated Raman spectra for all diamondoids analysed in this study are displayed in Figs. 2, 3, 6, 8–10. All modes in the calculated spectra are displayed as Lorentzians, each with a full-width half-maximum of 5 cm^{-1}. All spectra have been split into two groups, the higher frequency CH stretch region (2800–3100 cm^{-1}) and the lower frequency region. The CH stretch modes are approximately three times more intense than the other modes, and have been normalised to the strongest peak. The lower frequency region of the spectra are normalised to the strongest mode in the region 1100–1300 cm^{-1} not withstanding the occasional signal of high intensity at around 500 cm^{-1}.

Looking at the width of the bands corresponding to CH stretches compared to those associated with the lower frequency modes we find the CH stretching bands are considerably broader. This has been observed previously in adamantane [19] and was found to reduce considerably on cooling to below the plastic phase transition at 209 K. The cause of this broadening is unknown but is speculated to be caused by coupling of the high frequency modes to the crystal disorder.

The use of this level of theory and a split valence basis set to calculate vibrational frequencies and Raman activities of adamantane and its derivatives has been found to successfully reproduce experimental spectra [9,11]. Differences between the calculated and experimental spectra were found to be most pronounced in CH_2/CH bending vibrations, also noticed in our data. The causes of these deficiencies are uncertain but they are mostly likely due to use of a relatively small basis set or the effect of intermolecular interactions in the condensed phase.

3.1. Adamantane, diamantane, and triamantane

We start with the simplest example. Adamantane has 72 vibrational modes, $11T_2 + 7T_1 + 6E + 1A_2 + 5A_1$. The T_1 and A_2 vibrations are not Raman active, leaving 22 possible Raman signals. Comparing the experimental and calculated spectra (Fig. 2) we find that only half these modes are intense enough to be observable experimentally. The CH stretch region consists of six broad vibrations, three of which are so close in energy they are unresolvable (experimental frequency 2848 cm^{-1}, calculated frequency 3005 cm^{-1}, $E + A_1 + T_2$). The vibration with the highest Raman intensity is the fully symmetric A_1 mode (experimental frequency 2916 cm^{-1}, calculated frequency 3039 cm^{-1} and intensity 654 $Å^4$/amu). The lower wavenumber region contains five strong Raman bands, the most intense of which being the doubly-degenerate CH_2 twist mode (experimental wavenumber 1220 cm^{-1}, calculated wavenum-

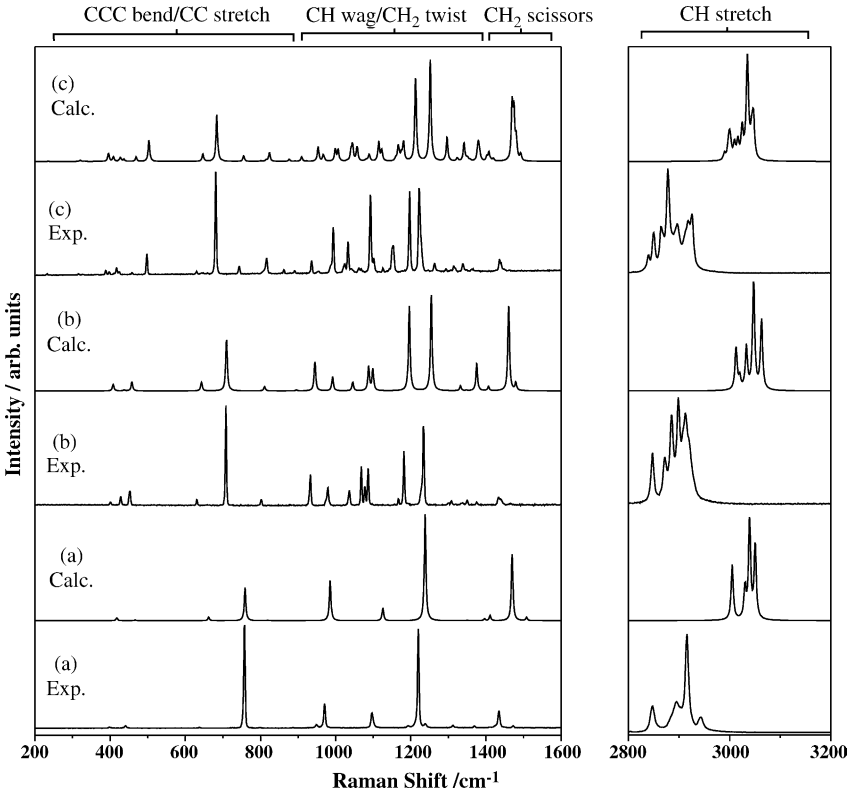

Fig. 2. Experimental and calculated spectra for (from bottom) adamantane (a), diamantane (b) and triamantane (c).

ber 1238 cm^{-1} and intensity 2×46 Å^4/amu). The other visible modes are the fully symmetric A_1 CC stretch (breathing) mode (experimental wavenumber 757 cm^{-1}, calculated wavenumber 759 cm^{-1} and intensity 27 Å^4/amu), a T_2 CC stretch/CCC bend mode (experimental wavenumber 971 cm^{-1}, calculated wavenumber 985 cm^{-1} and intensity 3×12 Å^4/amu), a T_2 CH_2 rock/CH wag mode (experimental wavenumber 1097 cm^{-1}, calculated wavenumber 1126 cm^{-1} and intensity 3×4 Å^4/amu) and finally an E CH_2 scissor mode (experimental wavenumber 1435 cm^{-1}, calculated wavenumber 1469 cm^{-1} intensity and 2×29 Å^4/amu).

Diamantane has 96 vibrational modes, $11A_{1g} + 6A_{1u} + 5A_{2g} + 10A_{2u} + 16E_g + 16E_u$. Only the A_{1g} and E_g species are Raman active, leaving 27 Raman active vibrational modes. Examining the experimental and calculated spectra (Fig. 2) we find 22 visible Raman signals. Comparing the adamantane and diamantane spectra we find similar broad high wavenumber CH stretch modes and the sharper lower wavenumber modes. Observing the CH stretch region we find that both have six Raman signals, produced by similar nuclear displacements, but in diamantane only two modes are close enough to be unresolvable, and hence giving the extra peak in the spectrum. Looking at the lower wavenumber range, there seems to be a reasonable correlation between the peak positions in the spectra of adamantane and diamantane, but there are more peaks present in the diamantane spectrum. For example, the single peak at 1220 cm^{-1} in the adamantane spectrum is replaced by two signals in the diamantane spectrum. Looking at the nuclear displacements associated with these vibrations, we find that all three are E_g modes consisting of CH_2 twisting motions strongly mixed with CH wagging modes. Both adamantane and diamantane have six CH_2 groups, and group theory shows that in both there should be only one E_g/E CH_2 twist. This suggests that the appearance of more in the spectrum must be due to mixing with extra CH wag/CC stretch E_g modes produced by the larger structure of diamantane. The majority of the peaks in the diamantane spectrum can be traced back to similar peaks in the adamantane spectrum, which have been complicated by mixing induced by extra modes of the same symmetry at similar energies.

The addition of another adamantane unit produces triamantane which has 120 vibrational modes, $35A_1 + 25A_2 + 29B_1 + 31B_2$. Again, the addition of another unit has reduced the symmetry of the molecule. From adamantane to diamantane this had little effect, as in both only some limited symmetries were Raman active. In triamantane, the symmetry has decreased to C_{2v}, so all modes are now Raman active, producing 120 possible signals in the Raman spectrum (Fig. 2). This increase in molecule size and decrease in symmetry means we now have 20 intense CH stretch vibrations in the same 100 cm^{-1} region, which produces a very poorly resolved experimental signal.

For the lower frequency region, the agreement between the experimental and calculated data appears to decrease. For adamantane and diamantane, the only major inconsistencies in the calculated intensities were the underestimation of the breathing modes (757 cm^{-1} in adamantane, 708 cm^{-1} in diamantane) and the overestimation of the CH_2 scissor modes (1435 cm^{-1}) relative to the ~1220 cm^{-1} CH_2 twist modes. As the complexity of the Raman spectra increases the deficiencies in the calculated

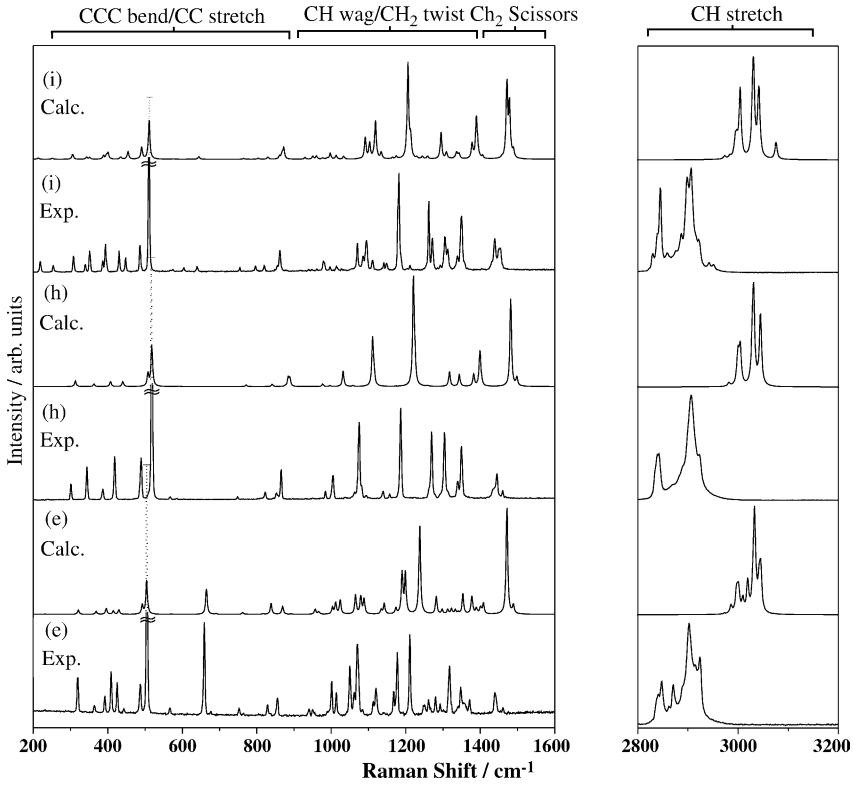

Fig. 3. Experimental and calculated spectra for (from bottom) [1(2)3] tetramantane (e), [1(2,3)4] pentamantane (h) and 3-methyl-[1(2,3)4] pentamantane (i). Spectra have been normalised to the most intense signal at ∼1200 cm^{-1}, higher intensity peaks are shown as dashed lines.

intensities become more prominent. The calculated spectrum for triamantane still has the same discrepancies as the adamantane and diamantane calculations but there is also disagreement in the intensity of vibrations in the region around ∼1300 and ∼1100 cm^{-1}. This type of disagreement is not wholly unexpected for calculations performed on molecules of this size due to the limitations in the size of basis set [11]. The most prominent signals in the low wavenumber region are two close peaks at 1197 and 1222 cm^{-1} similar to those observed in the diamantane spectrum, both of which are assigned to CH wag motions, and the 681 cm^{-1} cage deformation (CCC bend, CC stretch) which, again, also has an analogous peak in diamantane. As well as these modes there is a large abundance of weaker modes throughout the 400–1500 cm^{-1} region produced by the larger structure of triamantane and the absence of symmetry forbidden vibrations.

As mentioned above, the attachment of an additional adamantane unit to triamantane can occur in four distinct ways, producing two distinct molecules and a pair of enantiomers. In the next section, we shall study addition to the central unit in triamantane producing [1(2)3] tetramantane (e), and further addition to this to produce several pentamantane derivatives.

3.2. [1(2)3] Tetramantane, [1(2,3)4] pentamantane and 3-methyl-[1(2,3)4] pentamantane

The addition of an adamantane unit to the middle unit in triamantane produces [1(2)3] tetramantane ($C_{22}H_{28}$), trivially referred to as "*iso*-tetramantane". This increases the symmetry from C_{2v} to C_{3v}, meaning that of the 144 vibrational modes ($29A_1 + 19A_2 + 48E$), we would expect a maximum of 77 peaks in the Raman spectrum (Fig. 3), considerably less than for triamantane due to the presence of doubly degenerate E modes and the A_2 modes being Raman inactive in C_{3v} molecules. Despite the fewer expected signals there are still 15 intense CH stretch vibrations, again making this region of the spectrum poorly resolved. The lower wavenumber region does not have notably fewer peaks than triamantane, since although triamantane has 120 Raman active vibration modes not all of them will induce a significant change in polarisability in the molecule, necessary for an experimentally observable Raman signal. Again there are two intense E CH_2 twist modes (1177 and 1211 cm^{-1}) similar to those observed in the diamantane spectrum. But, as in the triamantane spectrum, the relative intensities of the neighbouring peaks are different in the calculated spectrum compared to the experimental spectrum. The most noticeable difference between the low wavenumber region of [1(2)3] tetramantane and the other diamondoid molecules studied so far is the increase in intense signals in the CCC bend/CC stretch deformation region. From adamantane to triamantane there has been only one strong signal, decreasing in wavenumber (from 757 to 681 cm^{-1}) as the molecular size increases. The same peak is still present in [1(2)3] tetramantane, but for the first time there are peaks with greater intensity at a lower wavenumber. The 659 cm^{-1} vibration involves stretching of the molecule parallel to the C_3 axis, whereas the more intense 505 cm^{-1} vibration is stretching perpendicular to this axis (Fig. 4). The experimental intensity of this perpendicular stretch is over twice as large as any other mode

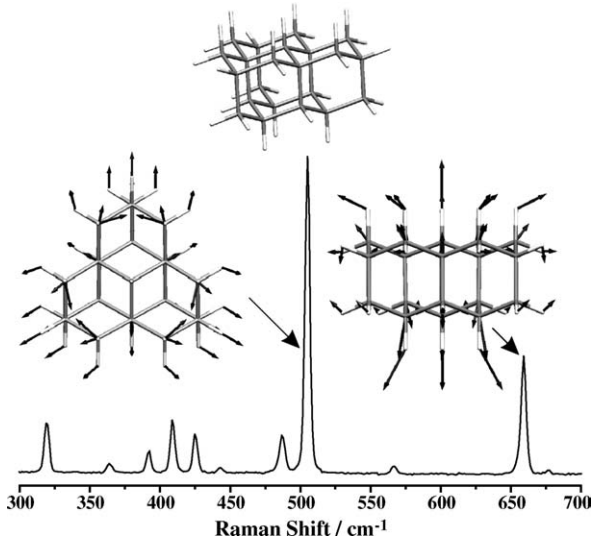

Fig. 4. Nuclear displacements of the 505 and 659 cm^{-1} modes of [1(2)3] tetramantane.

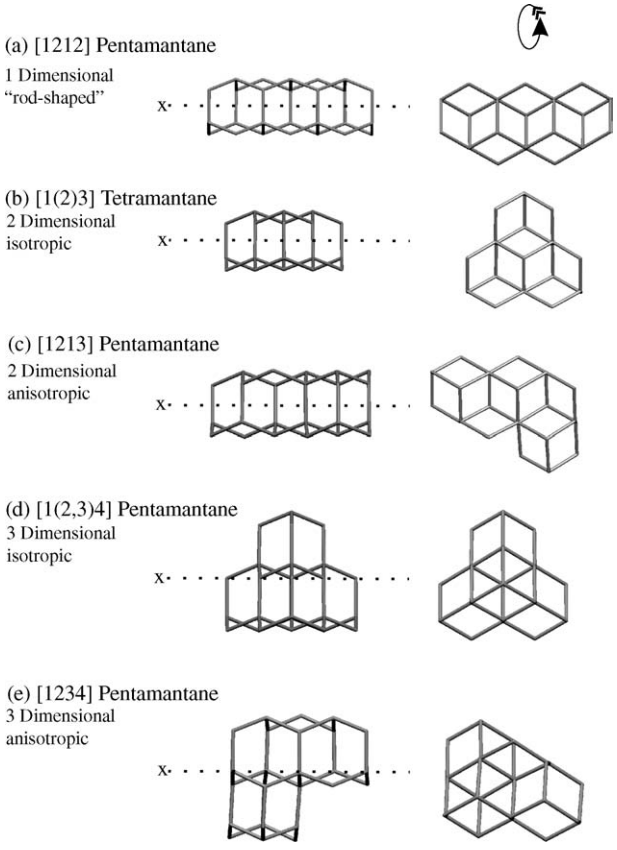

Fig. 5. The five diamondoid structural groups. The molecules on the right are identical to those on the left but rotated 90° around the *x*-axis, which is shown as a dotted line.

in the 200–1500 wavenumber region but in the calculated spectrum it is only half as intense as the strongest CH_2 twist mode. This appears to be another region where only limited accuracy can be achieved because of the large size of the systems. Peak assignment is still possible but the accuracy of the calculated vibrational frequencies is considerably better than the intensities.

As mentioned above, [1(2)3] tetramantane is formed by adding an extra unit to one of two equivalent sites on the central part of triamantane. Addition of a further unit to the other of these sites then leads to the smallest T_d symmetry polymantane after adamantane, [1(2,3)4] pentamantane ($C_{26}H_{32}$). [1(2,3)4] Pentamantane has 168 vibrational modes, $24T_2 + 18T_1 + 14E + 4A_2 + 10A_1$, but because of the double or triple degeneracy of some of the vibrations, and the T_1 and A_2 modes being Raman inactive, there is a maximum of 48 signals in the Raman spectrum (Fig. 3). The high symmetry of this particular polymantane suggests that it may be rewarding to compare its Raman spectrum to those of adamantane and [1(2)3] tetramantane. The CH stretch region of the Raman spectrum of [1(2,3)4] pentamantane contains eight vibrations which produces three broad peaks, bearing closer resemblance to the same region from adamantane than from [1(2)3] tetramantane. The CCC bend/CC stretch range, on the other hand, correlates better with that from [1(2)3] tetramantane. The only intense low wavenumber vibration in the adamantane spectrum occurs at 757 cm^{-1}, far from the 518 cm^{-1} mode in [1(2,3)4] pentamantane, whereas [1(2)3] tetramantane (as mentioned above) has both a peak at 659 and at 505 cm^{-1}. Up to [1(2,3)4] pentamantane, the Raman spectra of all diamondoids (with the exception of adamantane, a special case) have displayed a peak at or close to ~680 cm^{-1}. So what is it about the structure of [1(2,3)4] pentamantane that removes the Raman active vibrational mode at this wavenumber?

Looking at the structures of the diamondoid molecules in this study, we can put them all into one of five groups (Fig. 5). Diamantane and triamantane are both one-dimensional rod-shaped diamondoids (Fig. 5(a)) and would have the prefixes of [1] and [12] respectively, if they were not unique isomers. [1(2)3] Tetramantane is two-dimensional and has an isotropic structure i.e. symmetrical, disc-shaped (Fig. 5(b)). [1(2,3)4] Pentamantane is a three-dimensional isotropic diamondoid, its structure being a tetrahedral arrangement of five adamantane units. The peak occurring at ~680 cm^{-1} in all spectra except adamantane and [1(2,3)4] pentamantane is assigned as a breathing mode across a section which is one adamantane unit wide (Fig. 4 shows this for [1(2)3] tetramantane). [1(2,3)4] Pentamantane does not have a peak at ~680 cm^{-1} because it is not two-dimensional, there is no part of its structure that is only one-adamantane-unit across. Adamantane is a special case because all of its dimensions are one-adamantane-unit wide, and its equivalent peak is at 757 cm^{-1}, the lowest wavenumber strong Raman signal. The hypothesis that a strong peak at ~680 cm^{-1} can be used to identify a two-dimensional diamondoid (i.e. one whose structure is one-adamantane-unit wide) will be tested further as this study progresses.

Still looking at the low wavenumber region, both [1(2)3] tetramantane and [1(2,3)4] pentamantane display reasonably intense peaks below 450 cm^{-1} which only start to appear when the polymantane structure is large, due to vibrations featuring quaternary carbon CCC bending. Yet again, the most intense vibration in the low wavenumber region (excluding the breathing mode) is an E CH_2 twist mode.

For [1(2,3)4] pentamantane there are also discrepancies between the observed and calculated spectra in the ∼400 and ∼1300 cm^{-1} areas as observed for [1(2)3] tetramantane. It would be useful to see the effect of a larger basis set on the calculated spectrum but is not feasible on a molecule this size using B3LYP, but it is possible using Hartree–Fock. Recalculating the vibrational frequencies and Raman intensities of [1(2,3)4] pentamantane with Hartree–Fock theory and the same basis set, we find that the frequencies are considerably worse, but there is little change in the intensities. This suggests that correlation has little effect on calculated Raman intensities. If again we recalculate using Hartree–Fock with the larger 6-311+G(2d,p) basis set, we find that this does have a positive effect on the calculated intensities compared to the experimental data. The most obvious deviation in the smaller basis set calculation is the gross underestimation of the intensity of the 518 cm^{-1} breathing mode. In the experimental spectrum this mode is over twice as intense as any other in the non-CH stretch region, whereas in the smaller basis set calculation it is half as intense as the strongest mode. With the larger basis set, the calculated intensity of the breathing mode increases to be the strongest peak in the non-CH stretch region, a clear improvement over the smaller basis set calculation. In general, the overall "shape" of the larger basis set spectrum is significantly closer to the experimental than the smaller basis set, but there is still some disagreement. It would be useful to try even larger basis sets but it is not currently feasible for molecules as large as [1(2,3)4] pentamantane.

Recent work by Richardson et al. [18] used the Perdew–Burke–Ernzerhof generalized-gradient approximation (PBE) for the exchange and correlation functions and a very large basis set to study the Raman spectrum of [12312] hexamantane. The general shape of their calculated spectrum (intense breathing mode, weak CH_2 scissors) is considerably better than the one displayed here. Test calculations using the same PBE functional but the smaller SV basis set yield similar intensities to those obtained with B3LYP, suggesting that the accurate intensities produced by Richardson et al. are due to the basis set.

As well as [1(2,3)4] pentamantane we have also examined an alkylated version, 3-methyl-[1(2,3)4] pentamantane $C_{27}H_{34}$. Replacing the hydrogen atom at one of the apexes with a methyl group reduces the symmetry of the molecule to C_{3v} with the addition of only three atoms, increasing the number of vibrational modes by 9 to a total of 177, $36A_1 + 23A_2 + 59E$. Because of the reduction in symmetry the number of possible Raman signals increases from 48 to 95 (A_2 not active in C_{3v}), which is far more than might be expected from just the addition of three atoms. Comparing the spectra (Fig. 3) of these two molecules should give an insight to the effect of symmetry on a Raman spectrum. The reduction of symmetry is such that a T_2 symmetry vibration of a T_d molecule will give rise to two vibrations, of A_1 and E symmetry, in C_{3v}, while a T_1 vibration will give rise to two vibrations of A_2 and E symmetry. This shows how a near doubling of the number of Raman active vibrations results from the addition of three atoms. But do these new E symmetry modes created from T_1 modes induce a significant change in polarisability and hence produce new peaks in the spectrum? The overall shapes of the CH stretch regions of the two spectra are reasonably similar. The main differences are caused by the slight differences in frequency of the A_1 and E modes produced by the breaking of the T_2 modes by symmetry. There is also a small peak at ∼2950 cm^{-1} in the methyl-pentamantane spectrum due to the CH stretching mode of the CH_3 group. Studying the calculated frequencies and intensities in this region shows that there are Raman active modes of E symmetry that have gone over from inactive T_1 modes, but their intensities are low compared to the other CH stretch modes (∼30 times weaker than the most intense CH stretch). The lower frequency regions of the two spectra are remarkably similar, but again, there are a few cases of peak splitting. A prime example of this is the change from a single strong T_2 vibration at 1061 cm^{-1} in the [1(2,3)4] pentamantane spectrum to three E modes in the methylated pentamantane spectrum, which cannot easily be assigned as corresponding to T_1, T_2 or E modes of the T_d parent structure due to strong mode mixing.

3.3. [121] Tetramantane and [1212] pentamantane

The base tetramantane considered in this section is [121] tetramantane ($C_{22}H_{28}$, C_{2h}), trivially called "*anti*-tetramantane". [121] Tetramantane has 144 vibrational modes, $40A_g + 33A_u + 32B_g + 39B_u$, producing a maximum of 72 Raman fundamentals (Fig. 6) due to the inactivity of the B_u and A_u modes. The majority of the polymantanes remaining are large (≥50 atoms) with low symmetry (≤C_{2v}). Thus we ignore the CH stretch and CH_2 twist/CH wag modes due to the growing complication in extracting information from the increasingly large number of peaks in these regions. Instead, we shall concentrate upon the very low wavenumber modes (sub 800 cm^{-1}) as these are still easily resolvable and should be characteristic of the unique structural features of each diamondoid. All the diamondoids examined so far should be identifiable by using this lower wavenumber region as a fingerprint for the molecule, with the possible exception of [1(2,3)4] pentamantane and its alkylated derivative, which can be differentiated by the highest wavenumber mode in the CH stretch region. The polymantanes adamantane through to triamantane exhibit only one very intense mode below 800 cm^{-1}, so can be distinguished by the specific wavenumber of each mode. All others should be identifiable by a few relative peak intensities and positions.

Returning to [121] tetramantane, as with the other one- or two-dimensional diamondoids studied so far, there is a very strong peak at 680 cm^{-1}, but another interesting trend is also noticeable. Comparing the area around this peak in diamantane, triamantane, and [121] tetramantane, we find there is always a very weak accompanying peak ∼50 cm^{-1} lower which is absent in the spectrum of [1(2)3] tetramantane. If we look at the series of molecules, diamantane, triamantane and [121] tetramantane, (b)—(d) in Fig. 1, it is clear that on each occasion an adamantane unit is added to the end of the structure, producing the effect of "growing" the molecule in one direction. This leads to the conclusion that the appearance of this pair of peaks is an indication that the particular diamondoid is rod-shaped (group (a) in Fig. 5) i.e. its prefix would contain only alternating ones and twos. The nuclear displacements from the DFT calculations show that again the ∼680 cm^{-1} vibration is the same breathing

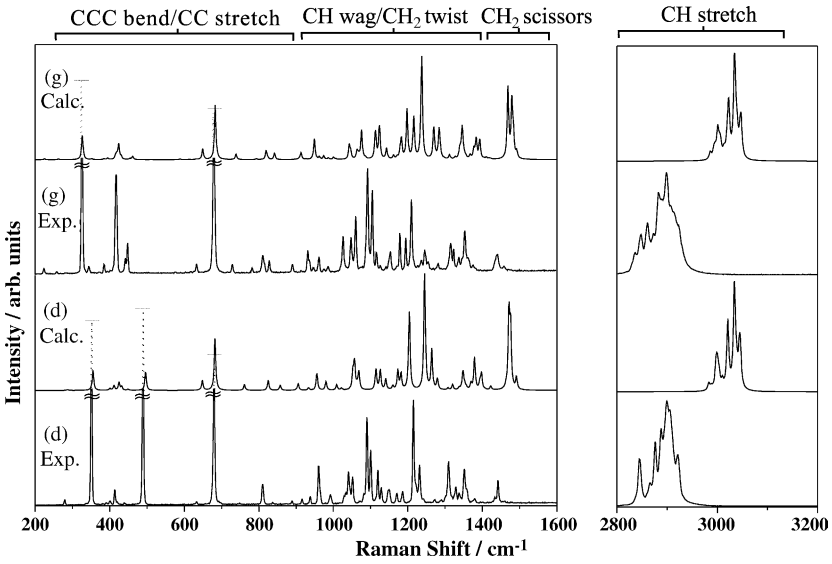

Fig. 6. Experimental and calculated spectra for (from bottom) [121] tetramantane (d) and [1212] pentamantane (g). Spectra have been normalised to the most intense signal at ~1200 cm^{-1}, higher intensity peaks are shown as dashed lines.

mode across a single adamantane unit, and its accompanying peak is also due to a CCC bend/CC stretch deformation at a different angle (Fig. 7), so both can only occur when the molecule is in this [1212...] group.

The only rod-shaped pentamantane is obtained by the addition of another unit onto the end of [121] tetramantane, and is called [1212] pentamantane ($C_{26}H_{32}$). This polymantane has 168 vibrational modes, $48A_1 + 36A_2 + 40A_1 + 44B_2$, all 168 being Raman active due to the C_{2v} point group (Fig. 6). Looking at the lower wavenumber regions of the two previous molecules, triamantane and [121] tetramantane, it is apparent that apart from some extra structure around the 426 cm^{-1} peak in [121] tetramantane, the only obvious difference is the relative intensity of the peaks at ~680 and ~500 cm^{-1}, with the former being far more intense in triamantane. The spectrum of [1212] pentamantane also satisfies the rule mentioned above, as it has a peak at ~680 cm^{-1} with a weaker companion ~50 cm^{-1} lower, which is characteristic of a rod-like structure.

There is also the ~426 cm^{-1} line caused by other deformations common to this linear structure. An interesting observation is a down-shifting in wavenumber of the 352 cm^{-1} peak present in [121] tetramantane to 325 cm^{-1} in [1212] pentamantane. The calculations show that this mode involves stretching of the molecule in the "growth" direction, hence a reduction in frequency is expected as the molecule becomes longer. What is surprising is the absence or weakness of this mode in triamantane compared to [121] tetramantane and [1212] pentamantane. The frequency of this particular mode may be a good indication of length of these rod-shaped diamondoids.

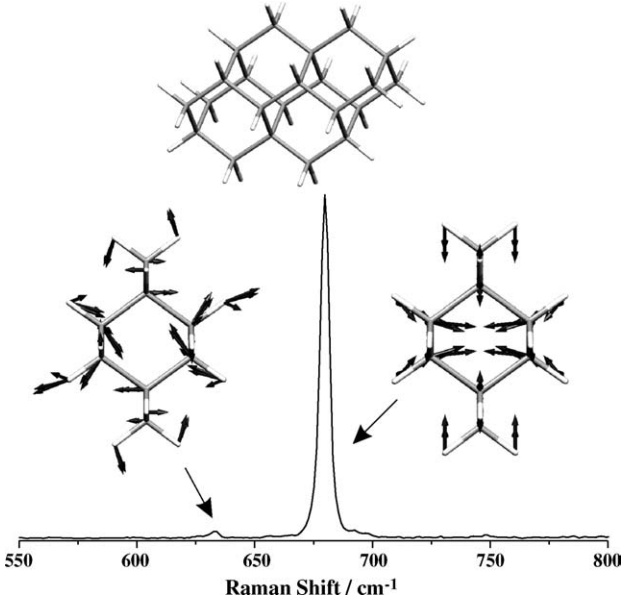

Fig. 7. Nuclear displacements of the 680 cm^{-1} mode and its companion mode in [121] tetramantane.

3.4. [123] Tetramantane and [1234] pentamantane

Addition of an adamantane unit to one of the four sites on triamantane not considered so far produces one enantiomer of the smallest chiral diamondoid, [123] tetramantane ($C_{22}H_{28}$, C_2), trivially called "*skew*-tetramantane". All 144 vibrational modes (73A + 71B) in [123] tetramantane are Raman active which explains why its spectrum (Fig. 8) is considerably more structured than those from the other tetramantanes. Even the 500–800 cm^{-1} region of the spectrum, which for the previous molecules is either free of signals (as in [1(2,3)4] pentamantane) or contains the two-dimensional or rod-shaped fingerprint peak (~680 cm^{-1}), is starting to display more signals. As expected, there is a single peak at 655 cm^{-1}, produced by the same breathing mode across a single adamantane unit ([123] tetramantane lies in the two-dimensional anisotropic group in Fig. 5). There is also the 516 cm^{-1} peak that appears in the other two tetramantanes which, in all cases, is related to the mode in [1(2)3] tetramantane (an expansion perpendicular to what would be the three-fold rotational axis in diamond). But now there are

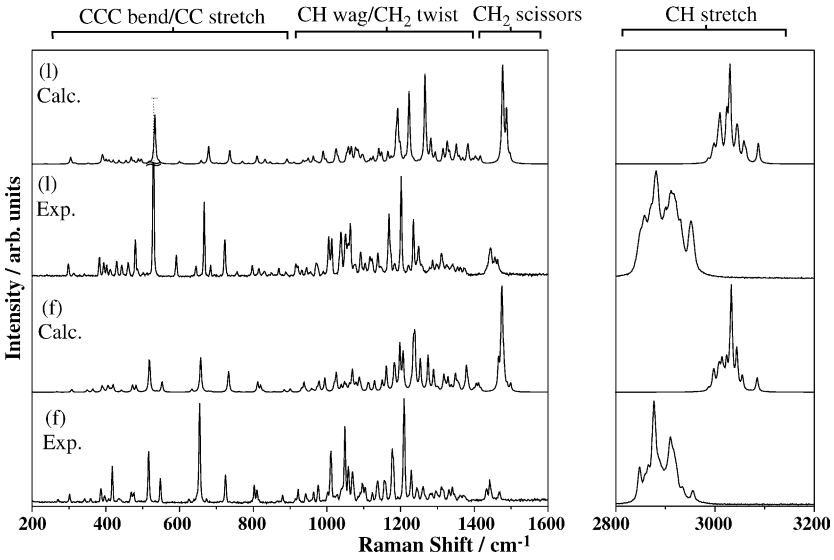

Fig. 8. Experimental and calculated spectra for (from bottom) racemic [123] tetramantane (f) and racemic [1234] pentamantane (l). Spectra have been normalised to the most intense signal at ∼1200 cm^{-1}, higher intensity peaks are shown as dashed lines.

other modes in this region, of a similar intensity to the 655 and 516 cm^{-1} modes. These modes are at 725 and 548 cm^{-1} and, again, are CCC bend/CC stretch deformations and are a feature of the more complex, less symmetrical structure of [123] tetramantane.

The chiral diamondoid [1234] pentamantane ($C_{26}H_{32}$, C_2) can only be formed by the addition of another adamantane unit to [123] tetramantane, and as the name suggests, extends the molecule in all three dimensions. This large, "screw-shaped", low symmetry molecule produces 168 vibrational modes (84A + 84B, all Raman active) again leading to a complicated spectrum (Fig. 8). As with [123] tetramantane there are several peaks in the 500–800 cm^{-1} region and, notably, the strong signal at 529 cm^{-1}. But unlike [123] tetramantane, where the intensity of these peaks was similar to the 516 cm^{-1} peak, in this case they are only approximately half as intense. These peaks are throughout the "structural fingerprint" region, which previously contained few peaks and was very descriptive of the structure of the molecule in question. The prefix to this molecule shows it extends in all three dimensions (like [1(2,3)4] pentamantane) but where this occurred previously there were no peaks in this region. This suggests that the fingerprint hypothesis requires some refinement, as follows.

For a three-dimensional isotropic structure, like the tetrahedron-shaped [1(2,3)4] pentamantane, the fingerprint region should be completely void of signals. The one-dimensional rod-shaped ([1212…] case) still stands, but there should be no strong signals in the region 500–800 cm^{-1} apart from the ∼680 cm^{-1} mode. An isotropic two-dimensional structure, like the disc-shaped [1(2)3] tetramantane, should only have the strong ∼680 cm^{-1} line. Complications arise when globally the molecule extends in three dimensions but there are local areas of two-dimensional structure. This is the three-dimensional anisotropic case (Fig. 5(e)), as in [1234] pentamantane. The same CCC bend/CC stretch motion that produces the single peak in the two-dimensional structures also occurs in these local two-dimensional structures, producing signals in the 500–800 cm^{-1} region of the spectrum that would not be seen for a solid three-dimensional structure. Using the relative intensities of the mode(s) at ∼680 cm^{-1} compared to that of neighbouring modes (i.e. the ∼500 cm^{-1} mode that appears in most spectra) it might be possible to tell the anisotropic three-dimensional molecules, that have only local two-dimensional structure, from the two-dimensional diamondoids, but the accuracy would be limited. This suggests that the fingerprint region of the spectrum is indeed diagnostic of isotropic three-dimensional, isotropic two-dimensional disc-shaped or one-dimensional rod-like structures. However, more care is needed for the more complicated diamondoid molecules.

3.5. [12(3)4] Pentamantane, [12(1)3] pentamantane and [1213] pentamantane

This section contains three diamondoids whose structures are as complicated, if not more complicated than the chiral pentamantane seen in the previous section. [12(3)4] Pentamantane ($C_{26}H_{32}$, C_s, 168 vibrational modes, 90A′ + 78A″, all Raman active) can be produced by addition to either [1(2)3] or [123] tetramantane. [12(1)3] Pentamantane ($C_{26}H_{32}$, C_1, 168 vibrational modes, 168 A, all Raman active), is produced by the addition of an adamantane unit to any of the three tetramantanes. [1213] Pentamantane ($C_{26}H_{32}$, C_1, 168 vibrational modes, 168 A, all Raman active), is produced by the addition of an adamantane unit to either [121] or [123] tetramantane. All these molecules have several peaks in the structural fingerprint region, and clearly do not fall into the rod-shaped, isotropic two-dimensional or isotropic three-dimensional categories. The prefixes specific to each molecule describe whether they are anisotropic two- or three-dimensional, but can this also be derived from the Raman spectrum?

Including [1234] pentamantane in this analysis allows the comparison of four spectra, two anisotropic two-dimensional

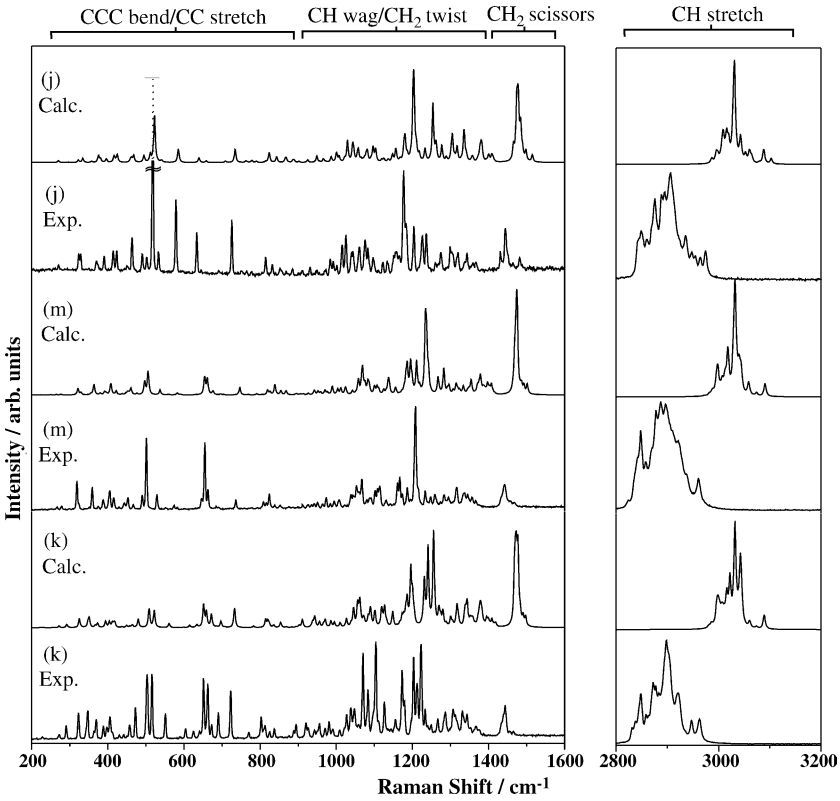

Fig. 9. Experimental and calculated spectra for (from bottom) racemic [1213] pentamantane (k) and racemic [12(1)3] pentamantane (m) and [12(3)4] pentamantane (j). Spectra have been normalised to the most intense signal at ~1200 cm^{-1}, higher intensity peaks are shown as dashed lines.

molecules (Fig. 5(c), e.g. [1213] and [12(1)3]) and two anisotropic three-dimensional molecules (Fig. 5(e), e.g. [1234] and [12(3)4]). The Raman spectra for all these molecules have several signals in the structural fingerprint region (Figs. 8 and 9), most due to single adamantane unit breathing vibrations in local regions of the molecules. Comparing the spectra of the two-dimensional molecules to the three-dimensional molecules there is a clear difference, but in relative Raman intensities rather than vibrational frequencies. In the spectra of the three-dimensional structures, the intensity of the 500 cm^{-1} mode (breathing parallel to the (1 1 1) face in diamond) is larger than any signal in the 200–1600 cm^{-1} region, whereas in the two-dimensional molecules spectra the intensities are similar. This suggests that just using this region of the spectrum it is possible to derive information, even when the diamondoid structure is complex, but this analysis is definitely becoming more difficult now that the molecules are very large and have the lowest symmetries, i.e. C_1 and C_s.

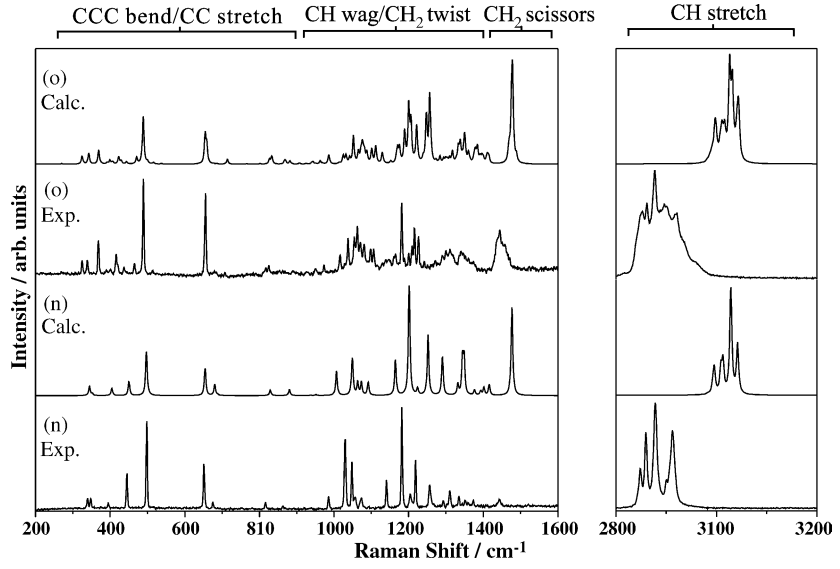

Fig. 10. Experimental and calculated spectra for (from bottom) [12312] hexamantane (n), and [121321] heptamantane (o).

3.6. [12312] Hexamantane and [121321] heptamantane

[12312] hexamantane (trivially called cyclohexamantane) and [121321] heptamantane could have been included in the [123] tetramantane section, being derivatives of only that particular tetramantane. But, as mentioned above, the pentamantane that lies between them ([1231] pentamantane) has not been isolated, possibly because of instability caused by the steric interaction between two of its hydrogen atoms. Because of this, and due to the relatively high symmetry of [12312] hexamantane, their Raman spectra shall be compared to the spectra of other diamondoids in a more general manner.

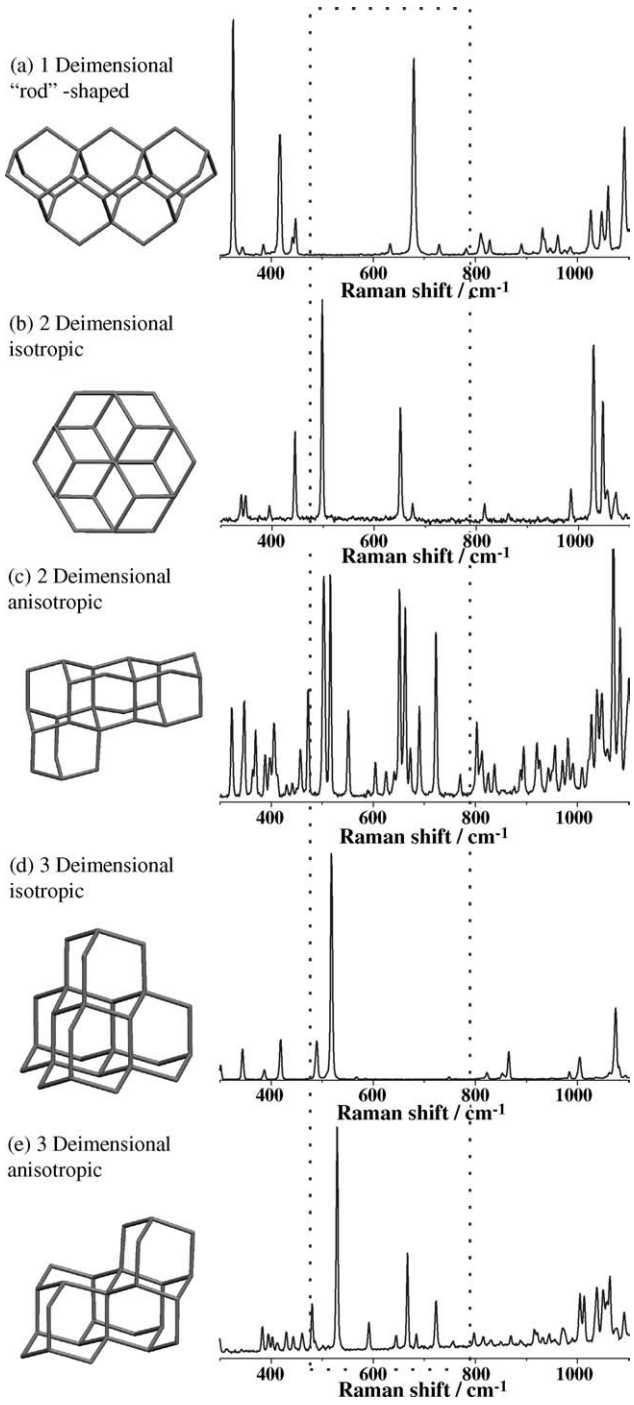

Fig. 11. Structural fingerprint region of, (a) one-dimensional rod-shaped [1212] pentamantane, (b) two-dimensional isotropic disc-shaped [12312] hexamantane, (c) two-dimensional anisotropic [1213] pentamantane, (d) three-dimensional isotropic [1(2,3)4] pentamantane, (e) three-dimensional anisotropic [1234] pentamantane.

Out of the 162 vibrational modes ($17A_{1g} + 11A_{1u} + 10A_{2g} + 19A_{2u} + 27E_g + 27E_u$), of [12312] hexamantane ($C_{26}H_{30}$, D_{3d}), only the $44E_g$ and A_{1g} symmetry modes are Raman active. The highest intensity mode in the lower frequency region is again a mixed CH wag/CH_2 twist mode of E symmetry at 1200 cm^{-1}, which is similar to those observed in the higher symmetry molecules mentioned above. The fingerprint region again has a peak at 651 and 498 cm^{-1} due to the same CCC bend/CC stretch deformations parallel to and perpendicular to the three-fold rotational axis as observed before in [1(2)3] tetramantane. [12312] Hexamantane has a two-dimensional isotropic disc-shaped polymantane structure, and that is clearly reflected in its Raman spectrum.

Adding another adamantane unit to [12312] hexamantane produces the largest diamondoid in this study, [121321] heptamantane ($C_{30}H_{34}$, C_s). This molecule has 186 vibrational modes ($100A' + 86A''$) all of them Raman active (Fig. 10). The Raman spectra of [12312] hexamantane and [121321] heptamantane are reasonably similar. There are many more peaks in the [121321] heptamantane spectrum but it does have an extra 142 Raman active vibrational modes so this is not surprising. It might be expected that as the diamondoid molecules become larger the addition of extra adamantane units would have less effect upon the Raman spectrum, until the only signal is the 1332 cm^{-1} phonon of the diamond crystal, but that is much greater than the size of molecules dealt with here. [121321] Heptamantane has low symmetry, but it has the same strong vibrational modes in the fingerprint region as [12312] hexamantane and is also two-dimensional.

4. Conclusions

In this paper, we report for the first time the experimental Raman spectra for a broad selection of diamondoid molecules ranging from adamantane to [121321] heptamantane. These spectra have been nearly completely assigned, by comparison with computed vibrational frequencies and Raman intensities derived from density functional theory computations. Calculated and experimental frequencies are generally in good agreement with each other, although some discrepancies arise between computed and observed intensities, mainly due to the relatively small atomic basis sets used.

Each diamondoid in this study produced a unique Raman spectrum, allowing for easy differentiation between molecules. The general features of the spectra allowed us to divide the diamondoids into five groups based on their molecular structure, with characteristic spectral properties for each group. Using only a small fingerprint region of the spectrum (550–700 cm^{-1}) we can identify to which group a specific diamondoid belongs, and hence gain information about its structure. The one-dimensional rod-shaped diamondoids (Fig. 11(a)) are identifiable by a single strong peak (~680 cm^{-1}) and weak companion peak (~50 cm^{-1}

lower) in this fingerprint region. The length of the rod can be estimated from the lowest wavenumber peak. Isotropic (symmetrical) two-dimensional diamondoids (Fig. 11(b)) should only have the single strong ∼680 cm^{-1} peak in the fingerprint region and should not have any weak signals between this peak and the strong ∼500 cm^{-1} signal. Anisotropic (low symmetry) two-dimensional diamondoids (Fig. 11(c)) may have several peaks in the fingerprint region but the ∼680 cm^{-1} peak should be weaker or as intense as the ∼500 cm^{-1} signal. If the ∼500 cm^{-1} peak is considerably more intense than the ∼680 cm^{-1} peak the diamondoid is three-dimensional anisotropic (Fig. 11(e)). The final group, three-dimensional isotropic, should have no peaks in the fingerprint region (Fig. 11(d)).

Acknowledgements

The authors would like to thank M. Kuball, A. Sarua and J. Pomeroy from the Bristol of University Physics Department for use of their Renishaw inVia system, F. Claeyssens for useful discussion and the EPSRC for funding.

References

[1] S. Landa, V. Machacek, Collect. Czech. Chem. Commun. 5 (1933) 1.
[2] S. HaIa, S. Landa, V. Hanus, Angew. Chem. Internat. Edit. 5 (1966) 1045.
[3] P.R. von Schleyer, G.A. Olah (Eds.), Cage Hydrocarbons, Wiley, New York, 1990, p. 138.
[4] V.Z. Williams Jr., P.R. von Schleyer, G.J. Gleicher, L.B. Rodewald, J. Am. Chem. Soc. 88 (1966) 3862.
[5] W. Burns, T.R.B. Mitchell, M.A. McKervey, J.J. Rooney, G. Ferguson, P. Roberts, J. Chem. Soc., Chem. Commun. 21 (1976) 893.
[6] E. Ozawa, A. Furusaki, N. Hashiba, T. Matsumoto, V. Sing, Y. Tahara, E. Wiskott, M. Farcasiu, T. Iizuka, N. Tanaka, T. Kan, P.R. von Schleyer, J. Org. Chem. 45 (1980) 2985.
[7] J.E. Dahl, S.G. Liu, R.M.K. Carlson, Science 299 (2003) 96.
[8] A.T. Balaban, P.R. von Schleyer, Tetrahedron 34 (1978) 3599.
[9] J.O. Jensen, Spectrochim. Acta A 60 (2004) 1895.
[10] P.W. May, S.H. Ashworth, C.D.O. Pickard, M.N.R. Ashfold, T. Peak, J.W. Steeds, Phys. Chem. Commun. (1998). Royal Society of Chemistry On-line Journal. http://www.rsc.org/is/journals/current/physchemcomm/contentslists/1998/pc998001.htm.
[11] L. Bistricic, L. Pejovb, G. Baranovic, J. Mol. Struct.-Theochem. 594 (2002) 79.
[12] A.C. Ferrari, J. Robertson, Phys. Rev. B 63 (2001) 121405(R).
[13] L. Bistricic, G. Baranovic, K. Mlinaric-Majerski, J. Mol. Struct. 508 (1999) 207.
[14] A. Kovacs, A. Szabo, J. Mol. Struct. 519 (2000) 13.
[15] L. Rivas, S. Sanchez-Cortes, J. Stanicova b, J.V. Garcia-Ramos, P. Miskovsky, Vib. Spectrosc. 20 (1999) 179.
[16] J.E.P. Dahl, J.M. Moldowan, T.M. Peakman, J.C. Clardy, E. Lobkovsky, M.M. Olmstead, P.W. May, T.J. Davis, J.W. Steeds, K.E. Peters, A. Pepper, A. Ekuan, R.M.K. Carlson, Angew. Chem. Int. Ed. 42 (2003) 2040.
[17] Y.F. Chang, Y.L. Zhao, M. Zhao, P.J. Liu, R.S. Wang, Acta Chim. Sinica 62 (2004) 1867.
[18] S.L. Richardson, T. Baruah, M.J. Mehl, M.R. Pederson, Chem. Phys. Lett. 403 (2005) 83.
[19] T.E. Jenkins, J. Lewis, Spectrochim. Acta 36A (1979) 259.
[20] T.E. Jenkins, A.R. Bates, J. Phys. C 12 (1979) 1003.
[21] M.J. Frisch, G.W. Trucks, H.B. Schlegel, G.E. Scuseria, M.A. Robb, J.R. Cheeseman, J.A. Montgomery Jr., T. Vreven, K.N. Kudin, J.C. Burant, J.M. Millam, S.S. Iyengar, J. Tomasi, V. Barone, B. Mennucci, M. Cossi, G. Scalmani, N. Rega, G.A. Petersson, H. Nakatsuji, M. Hada, M. Ehara, K. Toyota, R. Fukuda, J. Hasegawa, M. Ishida, T. Nakajima, Y. Honda, O. Kitao, H. Nakai, M. Klene, X. Li, J.E. Knox, H.P. Hratchian, J.B. Cross, C. Adamo, J. Jaramillo, R. Gomperts, R.E. Stratmann, O. Yazyev, A.J. Austin, R. Cammi, C. Pomelli, J.W. Ochterski, P.Y. Ayala, K. Morokuma, G.A. Voth, P. Salvador, J.J. Dannenberg, V.G. Zakrzewski, S. Dapprich, A.D. Daniels, M.C. Strain, O. Farkas, D.K. Malick, A.D. Rabuck, K. Raghavachari, J.B. Foresman, J.V. Ortiz, Q. Cui, A.G. Baboul, S. Clifford, J. Cioslowski, B.B. Stefanov, G. Liu, A. Liashenko, P. Piskorz, I. Komaromi, R.L. Martin, D.J. Fox, T. Keith, M.A. Al-Laham, C.Y. Peng, A. Nanayakkara, M. Challacombe, P.M.W. Gill, B. Johnson, W. Chen, M.W. Wong, C. Gonzalez, J.A. Pople, Gaussian 03, Revision B.04, Gaussian, Inc., Pittsburgh, PA, 2003.
[22] A. Schaefer, H. Horn, R. Ahlrichs, J. Chem. Phys. 97 (1992) 2571.